SHORT COMMUNICATION

Formation of tungsten-doped molybdenum selenide electrocatalyst for methanol oxidation reaction

Nabi Ullah[1] · Dariusz Guziejewski[1]

Abstract

Reaction medium (1,3-butane-diol) plays a vital role for the final morphology of W-$Mo_{15}Se_{19}$ electrocatalyst during synthetic strategy based on single-step solvothermal method. Smoothness of the electrocatalyst may govern its electrochemical application. High ECSA (0.055 mF/cm^2), low R_{ct}, low Tafel slope (99.0 mV/dec), and excellent long-term stability for 3600 s may attribute to its large surface area due to negligible agglomeration. W-$Mo_{15}Se_{19}$ delivers a current density of 1.65 mA/mg at an overpotential of 0.65 V (Ag/AgCl) in 0.75 M methanol and 1 M KOH, at a scan rate of 50 mV/s.

Keywords W-$Mo_{15}Se_{19}$ · Electrocatalyst · Microspheres · MOR · Alkaline

Introduction

Direct methanol fuel cells (DMFCs) exhibit low pollutant emission, low operating temperature, large conversion efficiency, and high availability of methanol as source of energy. Thus, DMFCs can be considered one of the future energy sources to reduce environmental pollution and energy crisis [1, 2]. It is also well-known that DMFC efficiency and reaction kinetics are strongly dependent on electrocatalytic materials of anode [3, 4]. In this regard, Pt is the state-of-the-art electrocatalyst for DMFCs to catalyze methanol electrooxidation reaction (MOR). However, sluggish kinetic, high price, and CO poisoning are main obstacles in their practical application [5, 6]. Thus, it is recommended to develop non-precious metal base active electrocatalyst for MOR.

Transition metal–based electrocatalysts exhibit high catalytic activity, corrosion resistance, and high conductivity [7]. Among these materials, molybdenum selenide exhibits high stability and thermoneutral energy. Additionally, molybdenum provides four electrons to selenium and a pair of electron is shielded at the selenium surface; this synergistic effect further improves the stability as well as activity of catalyst [8]. It is also well-known that the performance of bimetal is higher than single transition metal based electrocatalyst [9]. This enhancement of performance can be attributed to synergism of two metals [10].

Here, for the first time, tungsten-doped molybdenum selenide is developed via single step of solvothermal reaction for MOR application. The catalyst exhibits uniform spherical morphology with large surface area, high MOR activity, and high stability due to their negligible agglomeration.

Materials and methods

Synthesis

Simple solvothermal strategy was applied to prepare tungsten-doped molybdenum selenide electrocatalyst for MOR. Typically, 1.2 mmol of $(NH_4)_6Mo_7O_{24} \bullet 4H_2O$, 0.6 mmol of $Na_2WO_4 \bullet 2H_2O$, and 0.8 mmol of Na_2SeO_3 were simultaneously added to 30 mL of 1,3-butan-diol under vigorous stirring. Then, the mixture was transferred to a 50-mL stainless steel Teflon autoclave and heated for 16 h at 180 °C. After cooling down to room temperature, the sample was collected via centrifugation, washed with ethanol and water to remove impurities, finally dried at 60°C for overnight, and stored for further study.

Electrochemical study

A three-electrode setup linked with mAutolab potentiostat was utilized for electrochemical applications. Ag/AgCl, Pt rod, and glassy carbon electrode (GCE) were used as reference,

✉ Nabi Ullah
  nabi.ullah@chemia.uni.lodz.pl

[1] Department of Inorganic and Analytical Chemistry, Faculty of Chemistry, University of Lodz, Tamka 12, 90-403, Lodz, Poland

auxiliary, and working electrode, respectively. A total of 5 mg of electrocatalyst was dispersed in a mixture of 250 µL of ethanol and 750 µL of water, and ultrasonicated for 15 min to obtain a homogeneous composition. This freshly prepared suspension (2 µL) was drop casted on cleaned GCE surface and left to dry at ambient temperature; subsequently, 2 µL of Nafion was dropped on modified GCE surface and dried. This modified GCE was applied for electrochemical application in an alkaline medium (1 M KOH) with different methanol concentrations (0.25–1 M) at different scan rates (25–100 mV/s) via cyclic voltammetry (CV). Electrochemical impedance spectroscopy (EIS) was investigated at frequency range of $0.1\text{-}10^5$ Hz at open circuit potential with an AC amplitude of 5 mV. Chronoamperometry was recorded for 3600 s at potential of 0.6 V vs. Ag/AgCl. CVs were collected in the non-faradic region at scan rates 20–100 mV/s for the determination of electrochemical active surface area (ECSA) of the sample.

Characterization

Morphology of the electrocatalyst is confirmed by scanning electron microscopy (SEM) and transmission electron microscopy (TEM) via a scanning transmission electron microscope (STEM) (HR-SEM, Nova NanoSEM 450, FEI, Hillsboro, OR, USA, equipped with STEM II detector). The sample was also analyzed with energy-dispersive spectroscopy (EDS, EDAX/AMETEK, Materials Analysis Division, Model Octane Super, Mahwah, NJ, USA) to determine its purity and presence of elements. The sample was investigated with an X-ray diffractometer (XRD) (Aeris 1.2.0, Malvern Panalytical with Cu radiation and PIXcel 1D detector) for purity, phase, and crystallinity.

Results and discussion

Formation mechanism

$(NH_4)_6Mo_7O_{24}\bullet 4H_2O$ was dissolved in 1,3-butan-diol in the presence of tungsten and selenium salts. The molybdenum salt produced Mo^{6+} and ammonium ion and tungsten ions are released from its salt. Hussain et al. [11] confirmed that the presence of ammonium ion and organic solvent is critically imperative for final morphology of the electrocatalyst. Tungsten and molybdenum ions form complexes with organic solvent, and as the reaction proceeds, these
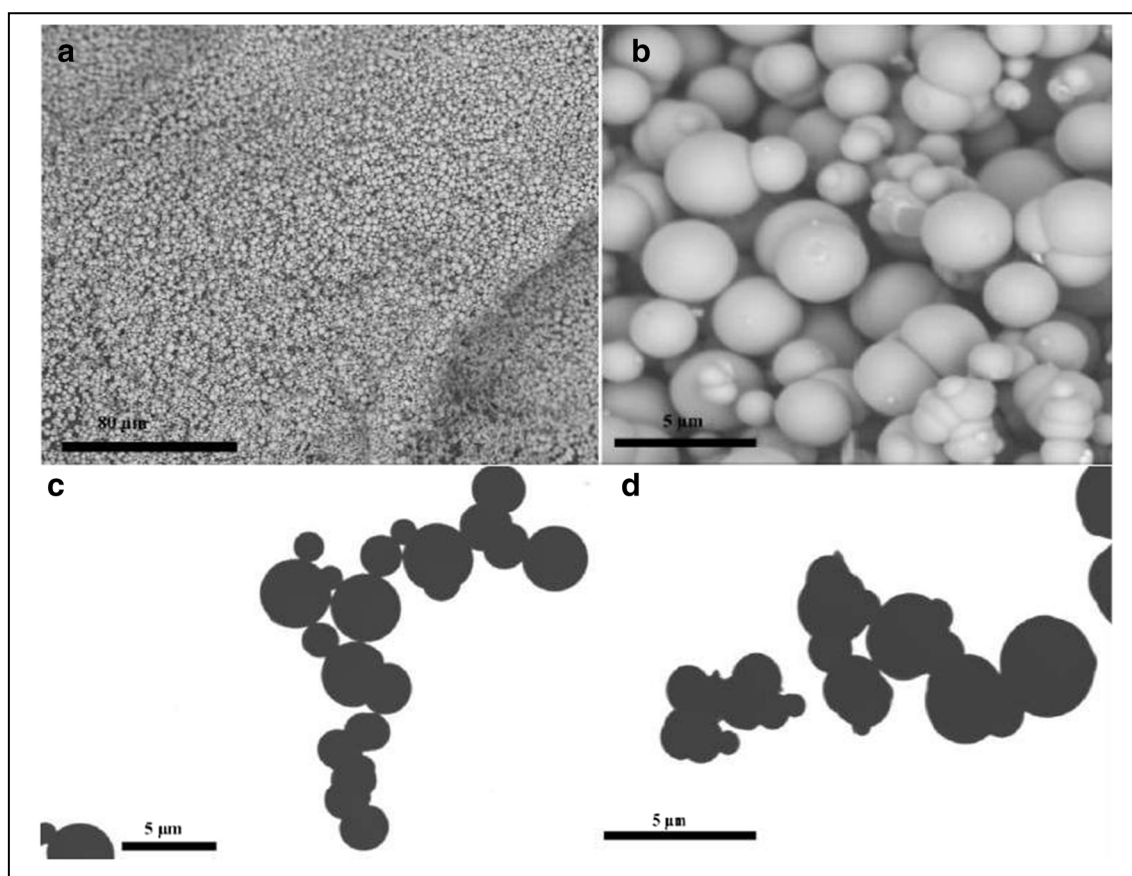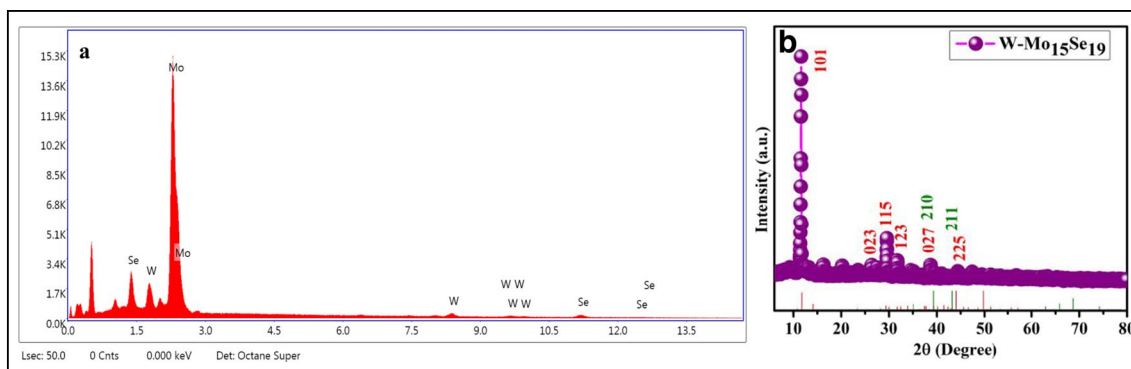

Fig. 1 a, b SEM and c, d TEM images of $W\text{-}Mo_{15}Se_{19}$

Fig. 2 **a** EDX and **b** XRD data of W-Mo$_{15}$Se$_{19}$ (at the bottom, the red line represents ICDD # 39-0786 and the green line represents ICDD # 41-1319)

complexes break down to release Mo ions, which reacts with Se to form molybdenum selenide; at the same time, W ion are also released and few of them replace Mo ions due to similar atomic size, or tungsten may set in space of molybdenum selenide crystal. The slow release of metal ions and high viscosity of the medium slow down the reaction and lead to multiple nucleation points. As reaction proceeds, more active atoms are released that are attached to nucleation centers and lead to micro-size, while ammonium ion and high viscosity dictate smooth surface of the material.
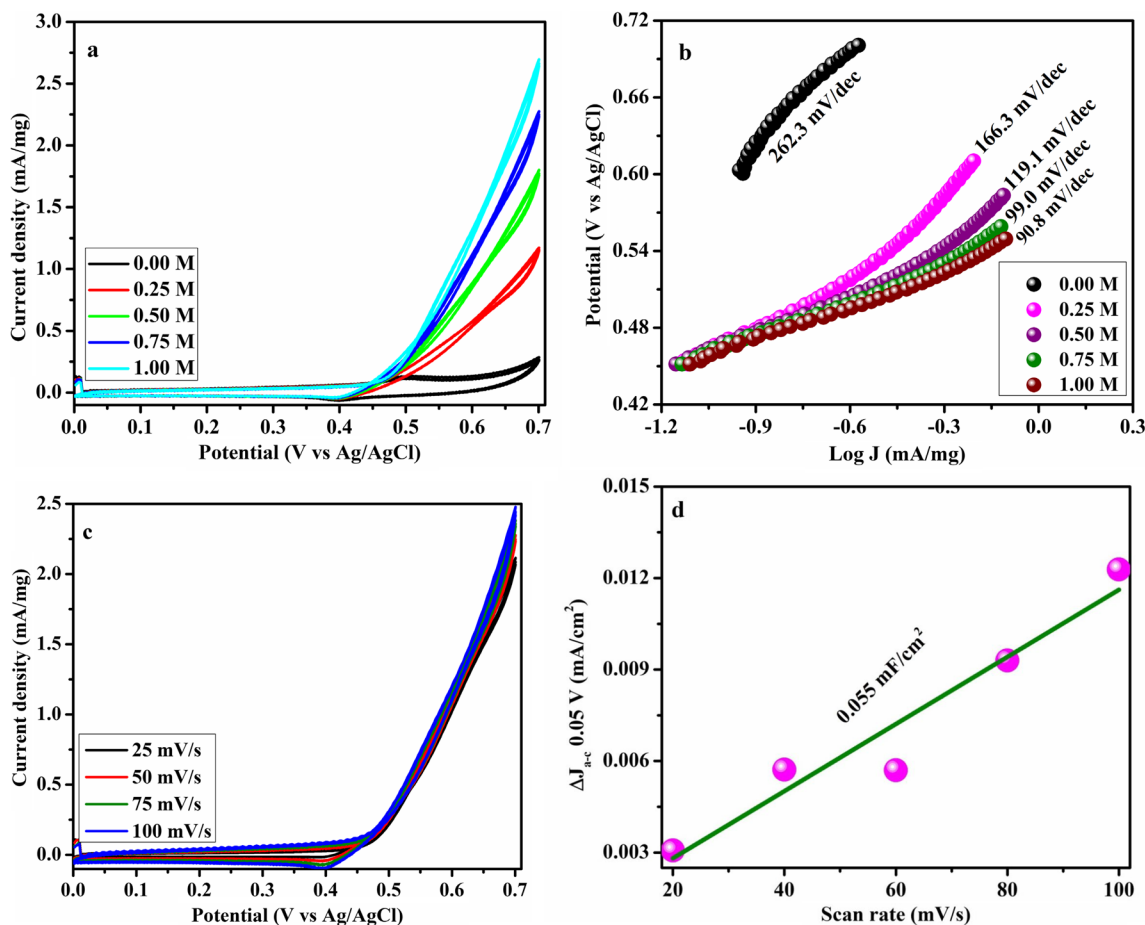

Fig. 3 CV cycles for MOR application in **a** 1 M KOH and 0.25–1M methanol at a scan rate of 50 mV/s, **b** Tafel slopes at different methanol concentrations, **c** effect of scan rate in 1 M KOH and 0.75 M methanol, and **d** ECSA of W-Mo$_{15}$Se$_{19}$ electrocatalyst

Morphology and purity

The SEM data (Fig. 1a, b) showed that the catalyst is composed of micro-spherical particles. The particles are well-developed, highly uniform, and negligibly agglomerated, and these features give high surface area to the materials. The smooth surface of the materials favors the fast release of oxide products after oxidation reaction of methanol is completed, providing space for the next target methanol molecules. The TEM data (Fig. 1c, d) supported the SEM data and revealed that the electrocatalyst is composed of microspheres with different sizes, uniform morphology, negligible agglomeration, and smooth surface, according to the formation mechanism.

The energy-dispersive X-ray (EDX) data (Fig. 2a) indicates that the electrocatalyst is mainly composed of Mo, W, and Se, confirming the sample's purity and formation mechanism. The XRD graph (Fig. 2b) shows sharp peaks at 11.2°, 26.0°, 29.1°, 31.6°, 38.3°, and 44.3° corresponding to fringes values of (101), (023), (115), (123), (027), and (225) corresponding to ICDD # 39-0786 of the hexagonal crystal of $Mo_{15}Se_{19}$. Very small peaks at 39.9° and 43.9° corresponding to fringes value of (210) and (211)

are well-matched with ICDD # 41-1319 of cubic crystal of tungsten. The very small intensity of the peaks is due to its very low concentration, as confirmed in energy dispersive x-rays (EDX) spectrum.

MOR application

Initially, the modified GCE was run in 1 M KOH solution for few cycles to get stabilized CV graph and then collect the data. The CV showed a small oxidation peak at 0.48 V (vs Ag/AgCl) but the response is very small in only KOH solution. When 0.25 M of methanol was added to 1 M KOH, the peak got increased instantly, which was further increased with 0.5 and 0.75 M methanol at a scan rate of 50 mV/s. Further increased to 1 M methanol, the response increased but comparatively low, as shown in Fig. 3a. Similarly, as the scan rate increased from 25 to 50 mV/s the response got increased, but at scan rates of 75 and 100 mV/s the enhancement in the current density is not very obvious, as shown in Fig. 3c. This data confirmed that 0.75 M methanol, 1 M KOH, and scan rate of 50 mV/s were optimized conditions to deliver a current density of 1.65 mA/mg at potential of 0.65 V (vs Ag/AgCl) with a Tafel slope of
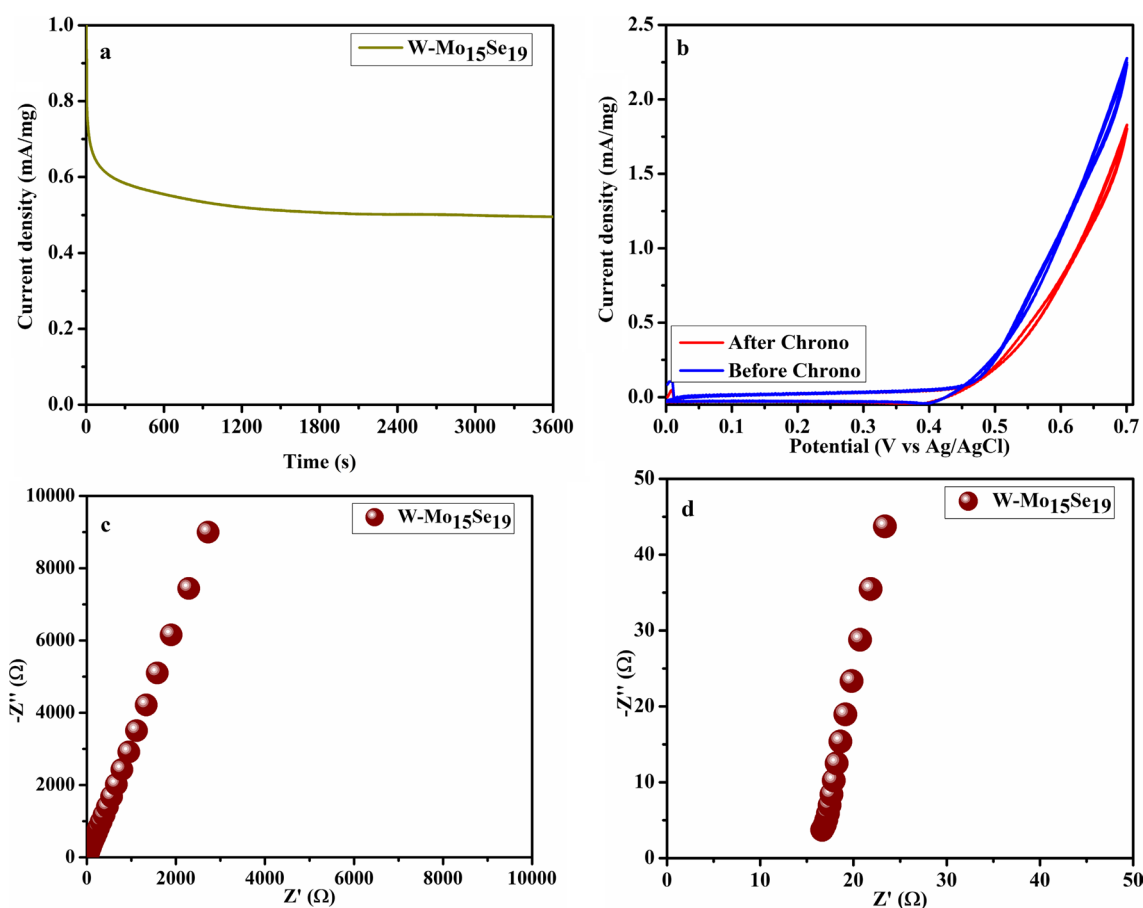

Fig. 4 **a** Chronoamperometry and **b** CV before and after chronoamperometry for stability determination. **c, d** EIS of W-$Mo_{15}Se_{19}$

99.0 mV/dec (Fig. 3b). The low response of the electrocatalyst may be due to low attachment feasibility of methanol molecules onto the smooth surface of the micro-spheres for the electro-oxidation reaction. The ECSA of the sample was calculated from CV recorded at scan rates of 20–100 mV/s using the double-layer capacitance (C_{dl}) method. The current density differences between anodic and cathodic current at potential of 0.05 V (vs Ag/AgCl) were plotted against scan rates and get a linear graph. The half of the slope of the graph is known as ECSA and was equal to 0.055 mF/cm^2 (Fig. 3d).

Stability is critically important for a catalyst; thus, the stability of the sample was determined by a chronoamperometric test collected in 0.75 M methanol and 1 M KOH solution at a potential of 0.6 V (vs Ag/AgCl) for 3600 s continuously. The electrocatalyst (Fig. 4a) showed almost negligible degradation for long-term usage in direct methanol oxidation reaction. The electrocatalyst was also compared before and after chronoamperometry, and the obtained CV showed very little change in the current density, as shown in Fig. 4b. EIS data was collected in 0.75 M methanol and 1 M KOH solution at a frequency range of 0.1–10^5 HZ, an AC amplitude of 5 mV/s, and an open circuit potential as initial potential. The data confirms that the electrocatalyst exhibits a negligible semi-circle (Fig. 4c) at a high frequency, which demonstrates the low charge transfer resistance of the electrocatalyst with electrolyte. Meanwhile, the almost horizontal line at low frequency demonstrates its good capacitive behavior may be due to low agglomeration, which favors high surface area, as shown in Fig. 4d.

It is revealed again that the sample exhibited high ECSA and low R_{ct} while its activity is governed by smooth surface of electrocatalyst, where it shows low attachment feasibility for methanol molecules to complete its electro-oxidation reaction.

Conclusion

W-Mo$_{15}$Se$_{19}$ electrocatalyst was prepared via single-step solvothermal method, where reaction medium (1,3-butane-diol) plays a vital role in the morphology of the sample. The surface of the sample is smooth and it may be the reason for diminished feasibility of methanol molecule attachment for oxidation reaction. The electrocatalyst exhibited high ECSA, low R_{ct}, and good long-term stability for 3600 s. The good MOR was obtained at optimized condition of methanol (0.75 M) and KOH (1 M) and a scan rate of 50 mV/s, where it delivered a current density of 1.65 mA/mg at an overpotential of 0.65 V (Ag/AgCl) with a Tafel slope of 99.0 mV/dec.

References

1. Lu Y, Tu J-p, Gu C-d, Xia X-h, Wang X-l, Mao SX (2011) Growth of and methanol electro-oxidation by gold nanowires with high density stacking faults. J Mater Chem 21(13):4843–4849

2. Hassan DK, El-Safty AS, Khalil KA, Dewidar M, Abu El-Maged G (2016) Mesoporous carbon/Co$_3$O$_4$ hybrid as efficient electrode for methanol electrooxidation in alkaline conditions. Int J Electrochem Sci 11(10):8374–8390

3. Wang H, Sun Z, Yang Y, Su D (2013) The growth and enhanced catalytic performance of Au@ Pdcore–shell nanodendrites. Nanoscale 5(1):139–142

4. Tian H, Zhu R, Deng P, Li J, Huang W, Chen Q, Su Y-Q, et al (2022) Ultrathin Pd$_3$Pt$_1$Rh$_{0.1}$ nanorings with strong C−C bond breaking ability for the ethanol oxidation reaction. Small 18(40):2203506

5. Tian H, Yu Y, Wang Q, Li J, Rao P, Li R, Du Y, et al (2021) Recent advances in two-dimensional Pt based electrocatalysts for methanol oxidation reaction. Int J Hydrogen Energy 46(61):31202–31215

6. Tian H, Wu D, Li J, Luo J, Jia C, Liu Z, Huang W, et al (2022) Rational design ternary platinum based electrocatalysts for effective methanol oxidation reaction. J Energy Chem 70:230–235

7. Liu G, Pan Z, Li W, Yu K, Xia G, Zhao O, Shi S, Hu G, Xiao C, Wei Z (2017) The effect of titanium nickel nitride decorated carbon nanotubes-reduced graphene oxide hybrid support for methanol oxidation. Appl Surf Sci 410:70–78

8. Burragoni SG, Koyyada G, Vattikuti SVP, Nam ND, Kim JH (2021) One-pot synthesis of flower-like MoSe$_2$ nanoflakes for photocatalytic hydrogen evolution and methanol oxidation. Mater Lett 282:128678

9. Gao H, Cao Y, Chen Y, Lai X, Ding S, Tu J, Qi J (2018) Au nanoparticle-decorated NiCo$_2$O$_4$ nanoflower with enhanced electrocatalytic activity toward methanol oxidation. J Alloys and Comp 732:460–469

10. Barakat NA, Motlak AM (2014) CoxNiy-decorated graphene as novel, stable and super effective non-precious electro-catalyst for methanol oxidation. Appl Catal B: Environ 154:221–231

11. Hussain I, Lamiel C, Sahoo S, Ahmad M, Chen X, Javed MS, Qin N, et al (2022) Factors affecting the growth formation of nanostructures and their impact on electrode materials: A systematic review. Mater Today Phys 27:100844

Publisher's note Springer Nature remains neutral with regard to jurisdictional claims in published maps and institutional affiliations.